Fabrication of gold nanostructures by templating from porous diatom frustules

Dusan Losic,*[ab] James G. Mitchell[b] and Nicolas H. Voelcker[a]

Received (in Montpellier, France) 5th January 2006, Accepted 23rd March 2006
First published as an Advance Article on the web 7th April 2006
DOI: 10.1039/b600073h

Diatoms produce diverse three-dimensional regular silica structures with nanometer to micrometer dimensions and hold considerable promise for biological or biomimetic fabrication of nanostructured materials and devices. In this paper, a simple procedure for fabrication of gold nanostructures with complex morphologies using porous diatom frustules as templates is described. The gold nanostructures are formed by means of thermal evaporation of gold onto porous frustules. Nanostructured gold films were obtained upon release from the diatom templates and were characterized using scanning electron microscopy (SEM), atomic force microscopy (AFM) and UV-Vis spectrophotometry. Three centric diatom species, *Coscinodiscus sp., Thalassiosira eccentrica* and one unidentified species cultured in our laboratory, were used as templates. The prepared gold replicas come in a variety of forms and shapes including arrays of nanoscale pillars, dots and more complex three-dimensional structures, depending on which porous surface of the diatom was used for replication. In all cases, gold nanostructures closely follow the organization and distribution of pores of the frustule template. Spectrophotometric characterisation shows that the templated nanostructured gold films exhibit localized surface plasmon resonance (LSPR) effects.

Introduction

Nanostructured materials are employed in manifold exciting areas of current research, the outcomes of which are applied across many disciplines.[1] In particular, considerable interest has been devoted to the noble-metal materials structured on the nanoscale, because of their unique physical and chemical properties.[2] Numerous studies have explored their applications as catalysts, sensors, and a new generation of optical, electronic, and magnetic devices.[2,3] Particular interest has been devoted to nanostructured gold.[4] Most of the existing nano- and microfabrication techniques have been applied to the fabrication of nanostructured gold; these include electron-beam lithography, laser ablation, electrochemical deposition, etching, template synthesis, and scanning probe microscopy.[5] Synthesis of materials using nanostructured templates has emerged as a popular and versatile technique to generate ordered nanostructures.[6] Templates consisting of porous membranes, zeolites, and crystalline colloidal arrays have been employed for the fabrication of a variety of nanoscale materials such as metals, semiconductors, metal oxides, carbon nanotubes, and polymers.[6,7] Fabrication of nanostructured gold substrates with nanoscale geometries that include wires, rods, tubes, rings and hollow structures using template synthesis has been reported.[8]

Biological materials and processes are a relatively new source of inspiration for the design and fabrication of advanced nanostructured materials.[9] Among existing microfabrication technologies, template synthesis using biological materials offers a convenient alternative for the fabrication of complex, spatially patterned micro-to-nano sized structures. There are numerous examples of organisms capable of synthesising inorganic based structures into intricate architectures with ordered features from the micro- to the nanoscale.[9] Recent reports have demonstrated the fabrication of metal nanostructures with a wide range of geometries (particles, wires, pores), using biomaterials as templates such as skeletal plates of echinoids (sea urchins), pollen grains, and cellulose fibers.[10]

Diatoms are single-celled photosynthetic microorganisms that possess intricate microshells (frustules) comprised of amorphous porous silica.[11] Because of their intricate silica-based architecture they are particularly attractive for nanofabrication. More so, because each of the more than 10^5 estimated diatom species has a specific frustule shape decorated with a unique porous pattern.[11] A plethora of potential applications for diatom frustules, including optics, biophotonics, electronics, biosensing, filtration, microfluidics, catalysis, lubrication and drug delivery have been proposed.[12] However, the conversion of the three-dimensional (3-D) biomineralised structure of a diatom frustule into technologically more suitable materials is essential for many of these applications. To transform biosilica into ceramic (MgO, TiO_2, zeolites), semi-conducting (Si–Ge) or organic scaffolds (polyaniline), several approaches have been demonstrated.[13,14] These include gas/solid displacement, sol-gel synthesis, polymerisation and genetic/environmental manipulation.[13–15]

In this paper, we present the approach of using the diatom frustule as a template for fabrication of gold nanostructures.[16]

[a] *School of Chemistry, Physics and Earth Science, Flinders University, Adelaide, SA 5042, Australia. E-mail: dusan.losic@flinders.edu.au; Fax: 08 8201 2905; Tel: 08 8201 2465*
[b] *School of Biological Science, Flinders University, Adelaide, SA 5042, Australia*

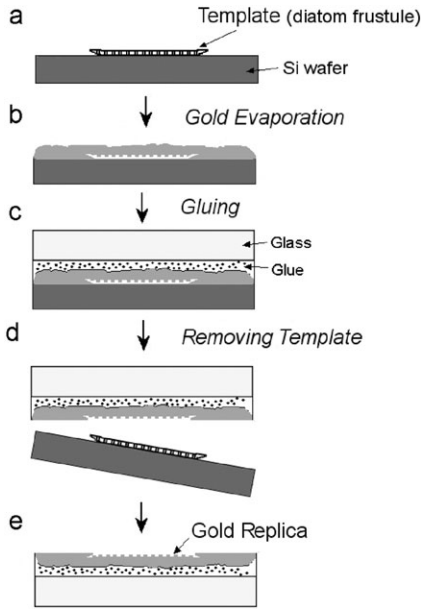

Fig. 1 Schematic for fabrication of gold nanostructures using diatom frustules as templates.

A schematic diagram of our fabrication approach is given in Fig. 1. The process starts by the thermal evaporation of gold on the diatom frustule, followed by stripping of the gold film. Evaporated gold condenses inside of the frustule pores (Fig. 1b), which results in the transformation of the pores into inverse gold structures (Fig. 1e). In comparison with previous studies, the focus of this method is on the preservation of the diatom nanotopography rather than on the replication of the curvature of the frustule valve. This approach is relevant to potential applications of gold nanostructures which rely on planar surfaces. The aims of this work are twofold, firstly, to demonstrate that templating using diatom frustules could be used as a generic approach for the fabrication of complex metal nanostructures. The second aim is to fabricate gold structures with intricate and unique morphologies that are not accessible by conventional fabrication techniques.

Experimental

Three diatom species, *Coscinodiscus sp*., *Thalassiosira eccentrica* (*T. eccentrica*) and one unidentified species (from the Derwent River in Hobart, Tasmania, Australia), were obtained from the CSIRO, Marine Division (Hobart, Tasmania, Australia). The cultures were maintained at 20 °C using a 12 hour light/12 hour dark cycle. GSE medium was used to culture *Coscinodiscus sp*. and Guillard's medium (f/2) was used for *T. eccentrica* and the unidentified species.[17] The live diatoms were harvested after 2–3 weeks of culturing and cleaned by concentrated sulfuric acid using a procedure described elsewhere.[18,19] This treatment also causes the separation of the diatom frustule into the two-frustule valves and girdle band. Unidentified diatom species were gently cleaned using 2% SDS in 100 mM EDTA followed by filtration and subsequent washing with distilled water. Cleaned frustule valves for both procedures were stored in 100% ethanol. One drop of the cleaned frustule suspension was deposited onto silicon wafers previously coated with polylysine (0.01% aqueous solution). Samples were dried under a gentle stream of nitrogen for 1 minute. Frustules settled on the substrate surface exposing their inner surface (concave) or exterior surface (convex) (Fig. 1a).

The evaporation of gold on the frustules template was performed using a custom-made vacuum evaporation system using procedures similar to those for fabrication of atomically flat gold described previously.[20,21] A silicon substrate was sandwiched into a mica holder and clipped on a heater inside the evaporation chamber. The substrate with its frustules was heated to approximately 50–100 °C for at least 1 hour before evaporation. Once the required vacuum was achieved ($< 1 \times 10^{-5}$ torr), gold was evaporated onto the substrate to form a continuous film with a minimum thickness of 1000 nm (Fig. 1b). To obtain a thicker gold film, two subsequent evaporations were performed without annealing. After cooling, the evaporated gold/diatom frustule substrates were removed from the chamber. The gold face was then glued to a solid support such as glass using either Torr Seal® (Varian Vacuum Products, Lexington, MA) or polyester glue (Cadillac Plastics Ltd., Australia) (Fig. 1c). The gold film was then mechanically stripped off the silicon wafer and the removal of the frustule from the gold was checked by light microscopy (Fig. 1e). In most cases, the frustule templates were removed from the gold and remained on the silicon wafer after stripping of the gold film. A small percentage of the frustules adhered to the gold layer, but could be easily removed by treatment with 6% HF. The resulting gold films after removal of frustule remains were rinsed with copious amounts of Milli Q grade water and dried under a stream of nitrogen. The structural characterisation of frustules and gold replicas was performed by scanning electron microscopy (SEM) and atomic force microscopy (AFM).

SEM imaging was performed using a Philips XL 30 operated at 2–10 kV and fitted with a field-emission source and energy-dispersive X-ray (EDX) analysis. Cleaned diatoms were deposited on silicon, coated with a thin platinum layer, and mounted on microscopy stubs with carbon sticky tape. The crystallinity of the prepared gold replica samples was investigated by the X-ray diffraction method (model Phillips PW-1730, Co K-alpha radiation, $\lambda = 1.7902$ Å).

AFM imaging of prepared diatoms and gold replica samples was performed using a Nanoscope IV Multimode SPM (Veeco Corp., Santa Barbara, USA). Tapping mode in air and ultrasharp (NT-MDT, Moscow, Russia) silicon tips with 150–350 KHz resonance frequencies were used. Different parts of the frustule including external and internal membrane layer and their corresponding gold replicas were characterized. Image processing was performed using Nanoscope off-line software (Veeco Corp., Santa Barbara, USA).

The absorbance spectra of the gold nanostructures were obtained using a CCD spectrometer (Ocean Optics, USB 2000, wavelength range 300–1000 nm) coupled through optical fibres to an optical microscope (40× objective corresponding to an illuminated area of less than 50 μm × 50 μm. The UV/Vis spectrum of the flat gold film was used as the background spectrum.

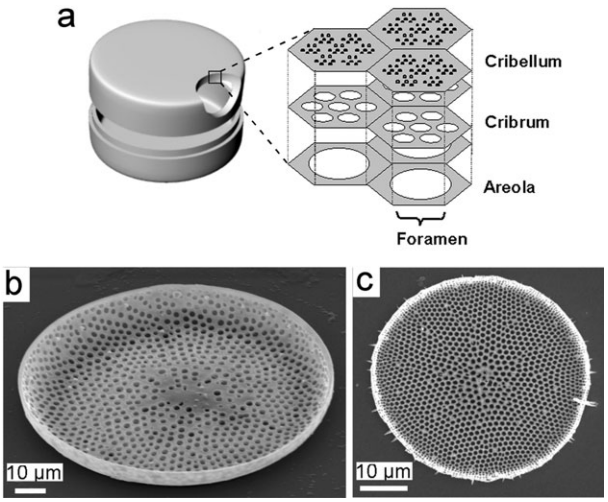

Fig. 2 (a) Schematic of a centric diatom frustule with a cross-sectional profile of the silica wall. SEM images of cleaned diatom frustules, (b) *Coscinodiscus sp*. and (c) *T. eccentrica*.

Results and discussion

The main morphological feature of diatoms is the frustule, a silica cell wall that consists of two valves, encasing the protoplasm, joined together by siliceous girdle bands. A schematic diagram of a common frustule structure of centric diatoms is shown in Fig. 2a. The frustule consists of a honeycomb of hexagonal chambers, called areolae. The areolae are capped on one side by one or two dense porous membranes (cribrum and cribellum). Cleaned frustules of two marine diatoms species *Coscinodiscus sp*. (size of 80–100 μm in diameter) and *T. eccentrica* (size of 30–60 μm in diameter) were used for this work.[22,23] Frustule valves of both species are shown in the SEM images of Fig. 2b–c. Both internal and external porous membrane layers were used as templates for fabrication of gold nanostructures.

A series of SEM and AFM images of the internal membrane of the *Coscinodiscus sp*. frustule used as templates are shown in Fig. 3a–e. The main feature of this membrane is radially organised pores (foramen openings) with an average diameter of about 1200 nm (Fig. 3b–e).[22,23] At the bottom of the foramen hole (Fig. 3c and d–e, arrow 1) smaller pores with a diameter of about 190 nm are clearly visible in both SEM and AFM images (Fig. 3c and 3d–e, arrow 2). These pores are part of the cribrum membrane, which is shown in the schematic of Fig. 2a. The distance between the top of the foramen hole and the cribrum pores was determined by AFM to be about 400 nm (profile graph, Fig. 3e).

SEM and AFM images of the gold replicas of corresponding sections on the diatom membrane are shown in Fig. 3. It is obvious that the shape, size, and organisation of gold structures represent the negative of the porous frustule valve used as the template. The gold replica film shows a complex 3-D morphology with two levels of ordered gold structures (Fig. 3i–j). The first are the large cylinder-like structures (arrow 1, Fig. 3i), with a height of about 400–500 nm (profile graph, Fig. 3j) and diameter about 1200 nm in consistency with the

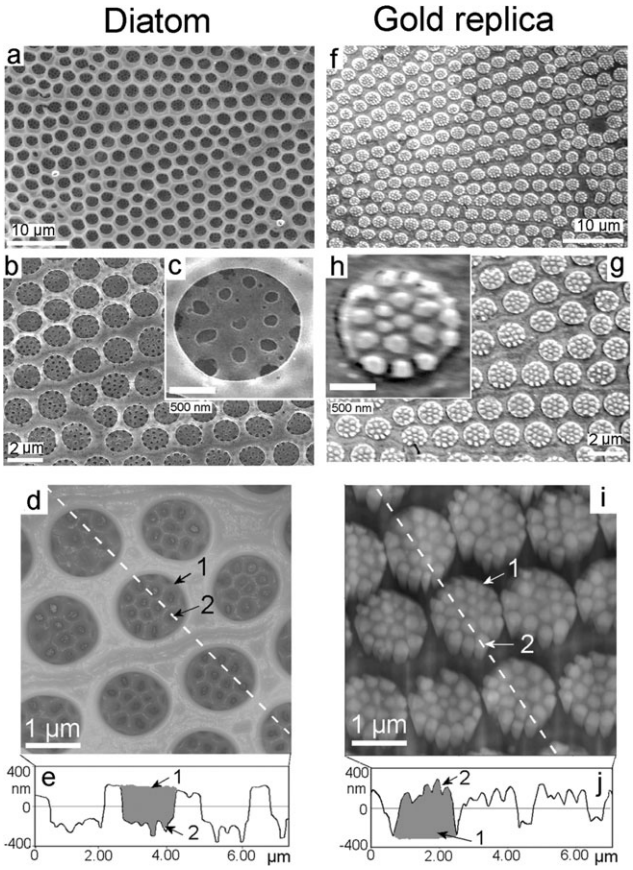

Fig. 3 A series of images of the internal frustule membrane of *Coscinodiscus sp*. used as template with corresponding gold replicas. (a–c) Low to high resolution SEM images of frustule; (d) AFM image of the internal membrane with profile graph (e) which shows the presence of two types of pores (arrow 1 is foramen, arrow 2 is cribrum); (f–h) low to high resolution SEM images of gold replicas; and (i) AFM image of gold replicas with corresponding profile graph (j) showing two gold structures (arrow 1 and arrow 2).

average diameter of the foramen holes (arrow 1, Fig. 3e). On top of these structures, an array of the smaller pillars with diameters of 200–300 nm and a height of 100–150 nm is seen (arrow 2, Fig. 3j). It is evident from the corresponding images that these small gold structures are conformal with the template pores (Fig. 3d–e). These comparative SEM and high resolution AFM images with profile graphs taken from both the template and the gold replica confirm precise and reproducible replication of the inner diatom membrane.

SEM images providing greater detail of the areolar chambers and the gold replica structures are shown in Fig. 4a–b. A high resolution SEM image of a single areolar chamber (Fig. 4b) nicely reveals the internal shape of the chamber with the cribrum membrane on the top (arrow 2) and the foramen perforation on the bottom (arrow 1). These images again corroborate that the 3-D structure of the gold replica constitutes a negative of the areolar chambers. The only exception is the curved shape of the frustule pore, which is not clearly seen in the gold replica. We observed that these individual gold structures could be removed from the gold film by gentle sonication. Removing and collecting these gold structures is

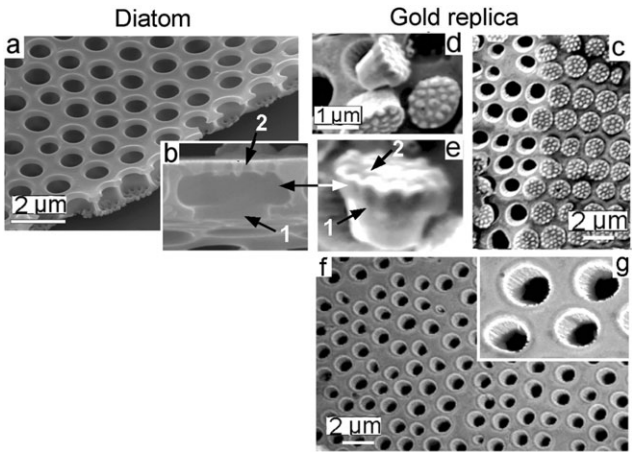

Fig. 4 (a–b) SEM images of multilayered valve of diatom frustule (*Coscinodiscus sp*.) showing profile structure of single areolar chamber; (c–e) SEM images of replicated gold nanostructures with 3-D morphology partially removed from gold film and (f–g) gold film with holes after removal of gold nanostructures.

another product of this approach in the fabrication of gold nanostructures with complex geometries (Fig. 4c–e). The profile image of a single gold structure is shown in Fig. 4e. It is apparent that the shape of this structure (arrow 2) is the negative of the templating areolar chamber (Fig. 4b). This unusual 3-D morphology of gold nanostructures might be of use to nanotechnological pursuits requiring monodisperse gold particle regimes. Complete removal of these ''nano-muffin'' like gold nanostructures results in a gold film with micron-sized pores (Fig. 4f–g).

A series of SEM and AFM images of the surface morphology of the frustule template from the external membrane (cribrum) of *Coscinodiscus sp*. and the corresponding gold replica structures are shown in Fig. 5. The structure of the cribrum is best described as a honeycomb of porous domes arranged in a hexagonal pattern (Fig. 5b–d). The porous silica membrane forming these domes is shown in more detail in Fig. 5d–f, which reveals two kinds of pores: firstly, pores with a diameter of about 200 nm (dashed arrow, Fig. 5f) and a density of 15–20 pores per dome. These pores are also seen through the foramen openings of the internal membrane shown in previous images (Fig. 3c–e). The second type of pores is an irregular shape with a diameter of 400–500 nm (full arrow, Fig. 5f), arranged in hexagons around the domes. These pores have been observed sporadically in diatom samples and their presence could be explained by suboptimal growth conditions or by damage during the cleaning process.

The images obtained of the gold replica fabricated from corresponding parts of the frustule are shown in Fig. 5g–l. Here, two arrays of structures of different size, but both following hexagonal arrangement are observed. The first smaller gold structures have a roughly conical shape with a diameter of about 200 nm and a height between 50–70 nm, whilst the second type of structures is roughly diamond-shaped with a size of about 500 nm and a height between 100–150 nm (Fig. 5i–j). The smaller gold structures correspond to the main cribrum pores seen in Fig. 5b–d whilst the bigger

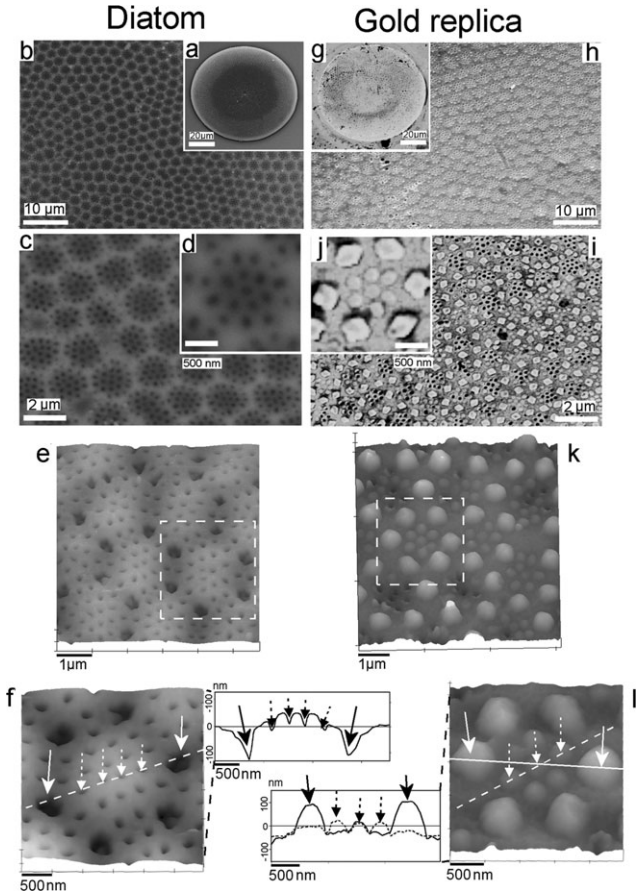

Fig. 5 A series of images of the external frustule membrane of *Coscinodiscus sp*. and the corresponding gold replicas; (a) SEM image from whole frustule and (b–d) images showing more details; (e–f) AFM images of the cribrum membrane with profile graph which shows two types of pores (full and dashed arrows). SEM images of corresponding gold replicas from whole diatom (g) and (h–j) images with greater detail; (k–l) comparative AFM images of gold structures replicated from cribrum membrane with profile graph showing two types of gold structures (full and dashed arrows).

gold structures are the results of templating from the large pores seen in Fig. 5e–f. This assignment was confirmed by high-resolution AFM of the cribrum frustule (Fig. 5e–f) and the gold replica (Fig. 5k–l). These images again show about 500 nm sized gold dots (full arrow, Fig. 5l) originating from large pores in the template (full arrow, Fig. 5f) and forming a corral around the smaller gold dots (dashed arrow, Fig. 5l), which correspond to the main cribrum pores (dashed arrow, Fig. 5f) in the template. However a disagreement in the number of small pores *vs*. small gold dots was also observed. On average 6–8 gold structures were seen in comparison with 15–20 pores per dome in the original frustule. This reduction in the numbers of replicated structures from the array of smaller pores is interesting, as we would have expected the evaporated gold film to be conformal to the silica membrane in a similar way to the process shown in Fig. 3d and 3i, where full replication is obtained. One could argue that only pores on top of the domes were successfully replicated, whilst the lower lying pores were not transformed into inverse gold structures

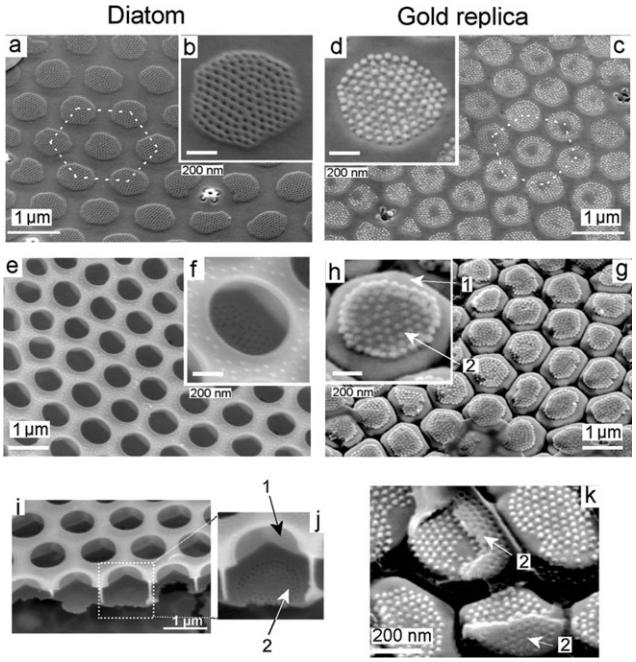

Fig. 6 Series of SEM images of the frustule *T. eccentrica* used as template and the corresponding gold replicas. (a–b) Low and high resolution images of internal frustule membrane with corresponding gold replicas on (c–d); (e–f) low and high resolution images of external frustule membrane with corresponding gold replicas on (g–h); (i–j) SEM images of the profile structure of frustule showing the pores from external (arrow 1) and internal membranes (arrow 2) and (k) silica remains (arrow 2) of the frustules partially removed from the gold replicas.

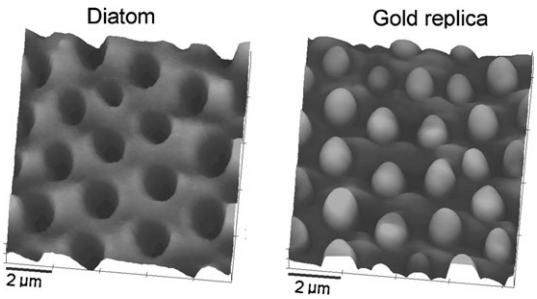

Fig. 7 AFM images (tapping mode in air) of (a) the external frustule of an unidentified diatom species (from the river Derwent, Tasmania) and (b) corresponding gold replica.

and that the curvature of the domes might prevent these features at the base of the dome from being resolved in the replica. Yet the spacing of the gold dots is not what would be expected if only some of the pores were replicated. We note that the reduced number of structures in the replica, compared to the original, shows a regular relationship to the nearest larger pores in the original. From this observation we propose that the nearby larger pores act as guides for the formation of the smaller structures. This hypothesis needs to be tested. However, if it is correct then our observation points the way to the use of guide structures to fabricate structures smaller than the guides and opens a path to fabrication of complex, regular gold structures of just a few nanometers.

To demonstrate that this method of templating can be used as a generic approach for the fabrication of metal (gold) nanostructures with a variety of shapes we have used a different diatoms species with a silica pattern distinct from *Coscinodiscus sp*. as the template. A series of gold replicas prepared using the frustule of *T. eccentrica* is shown in Fig. 6. Representative SEM images of the internal frustule layer in this diatom are shown in Fig. 6a–b. Characteristic arrays of pores (size of the array is 700–800 nm) arranged in hexagons with rather irregular boundaries are observed (Fig. 6a). Irregularities in the pore array shape (circular, ellipsoidal, quasi-rectangular) might be related to suboptimal culturing conditions.[19] The pores with an average diameter of about 40–50 nm are hexagonally packed (Fig. 6b) as the Fourier transform analysis confirms (data not shown). However, on occasions, undeveloped pores are visible, particularly in the central part of the wells.[22] The corresponding gold structures fabricated from this membrane are depicted in Fig. 6c–d. SEM images of the replica show an array of conical gold dots organised in the same pattern as the pores in the template. The diameter of these gold nanostructures at their base was found to be about 40–50 nm, and the height between 10–20 nm (determined by AFM) which is in perfect agreement with the size of the pores in the template. Some gold dots in the center of the arrays are missing, which are related to membrane replicas from samples with undeveloped pores.[22]

Representative SEM images of the external membrane of *T. eccentrica* are shown in Fig. 6e–f. This layer is composed of large, hexagonally packed pores (foramen) with a diameter of about 800 nm. Inside of the foramen opening, an array of smaller pores corresponding to the internal membrane of *T. eccentrica* could also be seen (Fig. 6f). SEM images of gold structures obtained from this template membrane are presented in Fig. 6g–h. They have 3-D structures that consist of platforms with roughly hexagonal shapes about 1000 nm long and decorated by aggregated gold dots (each *ca*. 50 nm in diameter) on the top. The size and shape of these dots (Fig. 6h) corresponds well with the dimensions of the pores of the internal layer (Fig. 6b) and they are similar in size to the dots observed on the gold replicas taken from the internal membrane (Fig. 6d). However, whilst the latter dots are free-standing and separated from each other, the dots seen in Fig. 6h are dispersed and separated by the remains of frustule silica.

In order to explain the shape of the platforms observed in the gold replica of Fig. 6g, SEM images of a broken *T. eccentrica* frustule were obtained (Fig. 6i–j). The profile structure of the areolar chamber confirms the presence of two pores (arrows 1 and 2). Interestingly, in contrast to the cylindrical chamber of *Coscinodiscus sp*. (Fig. 4a), the areolar chamber of *T. eccentrica* is of hexagonal shape, which explains the geometry of the gold structures in the replica seen in Fig. 6g. SEM images of partially removed frustule template show the remains of the internal silica membrane (arrow 2, Fig. 6k) and a piece of the silica wall structure (Fig. 6k). These results provide direct evidence for the origin of the observed topography of the gold replicas and prove that the internal surface of the frustule chamber is replicated into 3-D gold structures. Where

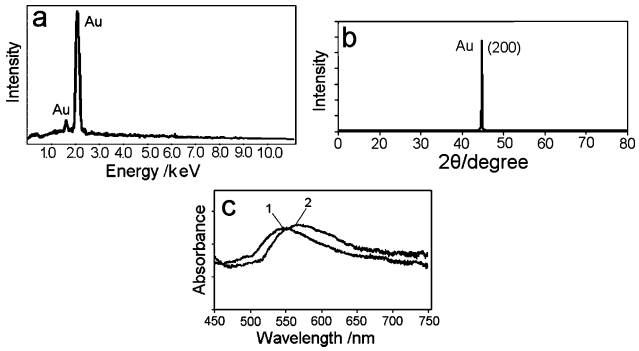

Fig. 8 (a) Typical EDX analysis of gold replicas, (b) XRD pattern of gold obtained from internal membranes of *Coscinodiscus sp*. and (c) UV/Vis absorbance spectra of the gold replicas obtained from the internal membrane of *T. eccentrica* (1) and external membrane of *Coscinodiscus sp*. (2).

the internal silica membrane was completely removed, arrays of gold dots similar to the ones depicted in Fig. 6d were observed.

The AFM images from the external membrane of an unidentified diatom species and its corresponding gold replica are shown in Fig. 7. The gold structures with cylindrical shape and size about 1.5 μm are in good agreement with the distribution, shape and size of the areolar pores of the diatom template. Interestingly in this case, featureless gold cylindrical structures were fabricated, unlike in the case of *Coscinodiscus sp*. and *T. eccentrica* where the underlying smaller porous membranes were also replicated. This is probably the result of gentle cleaning (surfactant) performed on this species which couldn't remove organic materials from internal pores.

The process of removing the gold film from templates by mechanical stripping in most cases was successful and no additional treatment by chemical dissolution of the remaining silica membranes was required. However, when templating from the internal frustule chamber (samples from *T. eccentrica)* the remains of thin silica structures were occasionally left as is seen in Fig. 6g–h and 6k, making their chemical removal necessary. Energy dispersive X-ray (EDX) analysis revealed only gold peaks (E = 2.12 keV) on the cleaned gold replica structures which confirms the purity of the gold, and the absence of silica (Fig. 8a).

In order to confirm the crystal phase of the gold replicas, X-ray diffraction (XRD) measurements were performed. An XRD spectrum of a gold replica is shown in Fig. 8b. A diffraction peak at $2\theta = 44.7^\circ$ was found which corresponds to Au(200) and face centered cubic phase of gold. Surprisingly, the Au(111) diffraction peak was not observed.

Application limitations of these gold replicas is their small lateral extent (30–100 μm in diameter). This limitation could be overcome in the future by using micromanipulators, optical tweezers or even self assembly tools to generate arrays of diatom frustules for subsequent templating.

Prepared gold replicas have ordered nanoscale features with dimensions comparable to the wavelength of visible light, which tempted us to probe their optical properties. Recent studies of nanometer sized gold structures demonstrated their localised surface plasmon resonance (LSPR) and surface enhanced Raman properties, which can be exploited in the development of highly sensitive devices for the detection of chemical or biological molecules.[24]

LSPR of gold nanoparticles arises from collective oscillation of the nanoparticle's conduction electrons when excited by electromagnetic radiation.[24] The LSPR response of the gold replica structures obtained from the external *Coscinodiscus sp*. membrane (Fig. 5g–l) and internal membrane of *T. eccentrica* (Fig. 6c–d) is shown in Fig. 8c. A peak (1) was observed with a maximum (λ_{max}) at 545 nm, which corresponds to the transverse plasmon absorbance band of the array of small gold structures (50 nm) observed in Fig. 6c–d. A second peak (2) with maximum (λ_{max}) at 565 nm corresponds to the gold replica with the array of two structures observed in Fig. 5g–l. These results show the shifting of the absorption peak toward larger gold nanostructures. The well-established chemistry of gold provides sufficient scope for further applications of these gold diatom replicas exploiting their unique structures and/or their optical properties. For example, gold is also one of the main electrode materials in electrochemistry and potential applications of these nanostructured gold films as micro- or nanoelectrode arrays or components of electrochemical or optical biosensors can easily be envisaged.

Conclusions

These results demonstrate that diatom frustules can be used as templates to fabricate gold structures with complex and unique morphologies. Gold replicas were prepared from frustule templates of two different diatom species, which suggests that the method may be used as a general approach. Diatoms can be routinely grown in laboratory conditions and this strategy offers a cheap resource to an enormous number of desired templates. Here, gold is used as an example, but the technique could be applied to many other metals that can be subjected to vacuum evaporation. This approach represents a worthy alternative to expensive lithographic procedures and results in complex 3-D nanostructures. In addition, we have shown that the fabricated gold nanostructures have characteristic optical properties, including LSPR, which could enable further applications, for example as components of biosensors.

Acknowledgements

The authors gratefully acknowledge support from Flinders University and the Australian Research Council. We thank the Ian Wark Research Institute, UniSA, for XRD measurement.

References

1 J. Jortner and C. N. R. Rao, *Pure Appl. Chem*., 2002, **74**, 1491.
2 N. L. Rosi and C. A. Mirkin, *Chem. Rev*., 2005, **105**, 1547.
3 (*a*) A. J. Haes and R. P. Van Duyne, *Anal. Bioanal. Chem*., 2004, **379**, 920; (*b*) Z. S. Li, C. X. Kan and W. P. Cai, *Appl. Phys. Lett*., 2003, **82**, 1392; (*c*) K. I. Bolotin, F. Kuemmeth, A. N. Pasupathy and D. C. Ralph, *Appl. Phys. Lett*., 2004, **84**, 3154.
4 C. W. Corti, R. J. Holliday and D. T. Toompson, *Gold Bull*., 2002, **35**, 111.
5 (*a*) Y. Kawakami, T. Seto, T. Yoshida and E. Ozawa, *Appl. Surf. Sci*., 2002, **197–198**, 587; (*b*) H. Chik and J. M. Xu, *Mater. Sci.*

Eng., 2004, **R43**, 103; (*c*) J. Erlebacher, M. J. Aziz, A. Karma, N. Dimitrov and K. Sieradzki, *Nature*, 2001, **410**, 450; (*d*) E. Irissou, B. Le Drogoff, M. Chaker, M. Trudeau and D. Guay, *J. Mater. Res*., 2004, **19**, 950.
6 S. Shingubara, *J. Nanopart. Res*., 2003, **5**, 17.
7 (*a*) M. Kruse, S. Franzka and G. Schmid, *Chem. Commun*., 2003, 1333; (*b*) J. Li, C. Papadopoulos and J. Xu, *Appl. Phys. Lett*., 1999, **75**, 367; (*c*) M. Steinhart, J. H. Wendorff and R. B. Wehrspohn, *ChemPhysChem*, 2003, **4**, 1171.
8 (*a*) C. R. Martin, *Chem. Mater*., 1996, **8**, 1739; (*b*) H. Masuda and K. Fakuda, *Science*, 1995, **268**, 1466; (*c*) S. Chah, J. H. Fendler and J. Yi, *J. Colloid Interface Sci*., 2002, **250**, 142; (*d*) D. Losic, J. G. Shapter, J. G. Mitchell and N. H. Voelcker, *Nanotechnology*, 2005, **16**, 2275; (*e*) F. Yan and W. A. Goedel, *Nano Lett*., 2004, **4**, 1193.
9 (*a*) M. Sarikaya, C. Tamerler, A. K.-Y. Jen, K. Scholten and F. Baneyx, *Nat. Mater*., 2003, **3**, 577; (*b*) M. Srinivasarao, *Chem. Rev*., 1999, **99**, 1935; (*c*) S. Weiner and L. Addadi, *J. Mater. Chem*., 1997, **7**, 689.
10 (*a*) S. R. Hall, H. Bolger and S. Martin, *Chem. Commun*., 2003, 2784; (*b*) F. C. Meldrum and R. Seshadri, *Chem. Commun*., 2000, 29; (*c*) J. He, T. Kumitake and T. Watanabe, *Chem. Commun*., 2005, 795.
11 F. E. Round, R. M. Craford and D. G. Man, *The Diatoms*, Cambridge University Press, Cambridge, 1990.
12 (*a*) D. E. Morse, *Trends Biotechnol*., 1999, **17**, 230; (*b*) R. W. Drum and R. Gordon, *Trends Biotechnol*., 2003, **21**, 325; (*c*) C. E. Hamm, *J. Nanosci. Nanotechnol*., 2005, **5**, 108; (*d*) T. Fuhrmann, S. Landwehr, M. E. Rharbi-Kucki and M. Sumper, *Appl. Phys. B*, 2004, **78**, 257; (*e*) N. L. Rosi, C. S. Thaxton and C. A. Mirkin, *Angew. Chem*., 2004, **116**, 5616.
13 K. H. Sandhage, M. B. Dickerson, P. M. Huseman, M. A. Caranna, J. D. Clifton, T. A. Bull, T. J. Heibel, W. R. Overton and M. E. A. Schoenwaelder, *Adv. Mater*., 2002, **14**, 429.
14 M. R. Weatherspoon, S. M. Allan, E. Hunt, Y. Cai and K. H. Sandhage, *Chem. Commun*., 2005, 651.
15 X. Li, C. Bian, W. Chen, J. He, Z. Wang, N. Xu and G. Xue, *Appl. Surf. Sci*., 2003, **207**, 378.
16 D. Losic, J. G. Mitchell and N. H. Voelcker, *Chem. Commun*., 2005, 4905.
17 R. R. L. Guillard and J. H. Ryther, *Can. J. Microbiol*., 1962, **8**, 229.
18 R. Hasle and G. A. Fryxell, *Trans. Am. Microsc. Soc*., 1970, **89**, 469.
19 M. S. Hale and J. G. Mitchell, *Aquat. Microb. Ecol*., 2001, **24**, 287.
20 D. Losic, J. G. Shapter and J. J. Gooding, *Langmuir*, 2001, **17**, 3307.
21 J. Mazurkiewicz, F. J. Mearns, D. Losic, L. Weeks, E. R. Waclawik, C. T. Rogers, J. G. Shapter and J. J. Gooding, *J. Vac. Sci. Technol., B*, 2002, **20**, 2265.
22 D. Losic, R. J. Pillar, T. Dilger, J. G. Mitchell and N. H. Voelcker, *J. Porous Mater*., 2006, in press.
23 D. Losic, G. Rosengarten, J. G. Mitchell and N. H. Voelcker, *J. Nanosci. Nanotechnol*., 2006, **6**, 982.
24 (*a*) A. J. Haes, L. Chang, W. L. Klein and R. P. Van Duyne, *J. Am. Chem. Soc*., 2005, **127**, 2264; (*b*) P. N. Bartlett, J. J. Baumberg, S. Coyle and M. E. Abdelsalam, *Faraday Discuss*., 2004, **125**, 117; (*c*) M. A. El-Sayed, *Acc. Chem. Res*., 2001, **34**, 257.

